Molecular Medicine

Liver Transplantation for Acute Intermittent Porphyria: Biochemical and Pathologic Studies of the Explanted Liver

Makiko Yasuda,[1] Angelika L Erwin,[1*] Lawrence U Liu,[2*] Manisha Balwani,[1,2] Brenden Chen,[1] Senkottuvelan Kadirvel,[1] Lin Gan,[1] M Isabel Fiel,[3] Ronald E Gordon,[3] Chunli Yu,[1] Sonia Clavero,[1] Antonios Arvelakis,[4] Hetanshi Naik,[1] L David Martin,[5] John D Phillips,[6] Karl E Anderson,[7] Vaithamanithi M Sadagoparamanujam,[7] Sander S Florman,[2,4] and Robert J Desnick[1]*

[1]Department of Genetics and Genomic Sciences, Icahn School of Medicine at Mount Sinai, New York, New York, United States of America; [2]Department of Medicine, Icahn School of Medicine at Mount Sinai, New York, New York, United States of America; [3]Department of Pathology, Icahn School of Medicine at Mount Sinai, New York, New York, United States of America; [4]Department of Surgery, Icahn School of Medicine at Mount Sinai, New York, New York, United States of America; [5]Department of Medicine, Johns Hopkins University School of Medicine, Baltimore, Maryland, United States of America; [6]Department of Internal Medicine, University of Utah, Salt Lake City, Utah; and [7]Department of Preventive Medicine and Community Health, University of Texas Medical Branch, Galveston, Texas

Acute intermittent porphyria (AIP) is an autosomal-dominant hepatic disorder caused by the half-normal activity of hydroxymethylbilane (HMB) synthase. Symptomatic individuals experience life-threatening acute neurovisceral attacks that are precipitated by factors that induce the hepatic expression of 5-aminolevulinic acid synthase 1 (*ALAS1*), resulting in the marked accumulation of the putative neurotoxic porphyrin precursors 5-aminolevulinic acid (ALA) and porphobilinogen (PBG). Here, we provide the first detailed description of the biochemical and pathologic alterations in the explanted liver of an AIP patient who underwent orthotopic liver transplantation (OLT) due to untreatable and debilitating chronic attacks. After OLT, the recipient's plasma and urinary ALA and PBG rapidly normalized, and her attacks immediately stopped. In the explanted liver, (a) *ALAS1* mRNA and activity were elevated approximately ~3- and 5-fold, and ALA and PBG concentrations were increased ~3- and 1,760-fold, respectively; (b) uroporphyrin III concentration was elevated; (c) microsomal heme content was sufficient, and representative cytochrome P450 activities were essentially normal; (d) HMB synthase activity was approximately half-normal (~42%); (e) iron concentration was slightly elevated; and (f) heme oxygenase I mRNA was increased approximately three-fold. Notable pathologic findings included nodular regenerative hyperplasia, previously not reported in AIP livers, and minimal iron deposition, despite the large number of hemin infusions received before OLT. These findings suggest that the neurovisceral symptoms of AIP are not associated with generalized hepatic heme deficiency and support the neurotoxicity of ALA and/or PBG. Additionally, they indicate that substrate inhibition of hepatic HMB synthase activity by PBG is not a pathogenic mechanism in acute attacks.

Online address: http://www.molmed.org
doi: 10.2119/molmed.2015.00099

INTRODUCTION

Acute intermittent porphyria (AIP), the most common acute hepatic porphyria, is an autosomal-dominant disorder due to the half-normal activity of the heme biosynthetic enzyme, hydroxymethylbilane (HMB) synthase (1). Symptomatic heterozygotes, most (~90%) of which are women, experience episodic life-threatening acute neurovisceral attacks that typically begin with severe abdominal pain and may include hypertension, tachycardia, constipation, motor weakness and seizures. These attacks are precipitated by certain drugs, dieting and hormonal factors that increase the hepatic expression of 5-aminolevulinic acid synthase 1 (*ALAS1*) (1). When hepatic ALAS1 is induced, the half-normal activity of HMB synthase becomes rate-limiting, leading to decreased heme biosynthesis and depletion of the hepatic "free" heme pool. Depletion of the"free" heme pool leads to further induction of

**MY, ALE, and LUL contributed equally to this work.*

Address correspondence to *Robert J Desnick, Department of Genetics and Genomic Sciences, Icahn School of Medicine at Mount Sinai, 1425 Madison Ave., Room 14-34, New York, NY 10029. Telephone: 212-659-6700; Fax: 212-360-1809; E-mail: robert.desnick@mssm.edu.*

Submitted May 1, 2015; Accepted for publication June 4, 2015; Published Online (www.molmed.org) June 5, 2015.

The Feinstein Institute for Medical Research
North Shore LIJ
Empowering Imagination. Pioneering Discovery.®

hepatic *ALAS1* expression and increased production and accumulation of the porphyrin precursors aminolevulinic acid (ALA) and porphobilinogen (PBG) (1).

The current approved treatment for the acute attacks is intravenous hemin infusions, which provide sufficient "free" heme to downregulate hepatic ALAS1 activity, leading to decreased production of ALA and PBG. Patients suffering recurrent attacks (particularly women who have cyclic attacks with their menstrual cycles) may be treated prophylactically with weekly to monthly hemin infusions and/or gonadotropin-releasing hormone analogs to prevent ovulation. However, recurrent attacks are often difficult to control and may result in chronic symptoms, particularly chronic neuropathic pain and progressive neuropathy that markedly impair the quality of life (1). Recently, orthotopic liver transplantation (OLT) was performed on several AIP patients in Europe who failed medical management for their recurrent severe attacks (2–6). Patients who were successfully transplanted normalized their urinary ALA and PBG levels and have remained attack-free up to 10 years after transplantation (3,5).

Two major hypotheses regarding the pathobiology of the acute attacks have been proposed: first, the hepatic metabolites ALA and/or PBG are neurotoxic and, second, heme deficiency leads to decreased neuronal hemoprotein production and causes the acute neurovisceral symptoms (7). The success of OLT in treating these severely affected AIP patients demonstrated that the liver is the major etiologic site of pathology and strongly supports the hypothesis that the markedly increased levels of ALA and/or PBG are the primary mediators of the acute attacks. In further support of this concept, when the explanted livers of AIP patients were transplanted into nonporphyric recipients with hepatocellular carcinoma (that is, "domino" liver transplants), recipients developed acute porphyric attacks characterized by increased urinary ALA and PBG levels (8). However, the contribution of generalized heme deficiency to disease pathogenesis is not entirely clear, since hemoprotein function in human AIP tissues during an acute attack have not been reported.

Here we describe the clinical and biochemical effects of the first OLT in the Americas for a severely affected AIP patient and document in detail the relevant biochemical and pathologic abnormalities in the explanted porphyric liver. Unlike previous reports in which only daily urinary ALA or PBG levels were obtained, plasma and urinary ALA and PBG concentrations were monitored frequently after transplantation to determine the kinetics of the toxic metabolite clearance. The data presented are the first from the liver of an AIP patient with debilitating and continuous symptoms, and they provide evidence that the hepatic overproduction and neurotoxic effects of ALA and/or PBG account for the neurovisceral manifestations.

MATERIALS AND METHODS

Collection of Human Tissues and Body Fluids

Small pieces of the explanted AIP liver (~5 g) were snap-frozen in liquid nitrogen and stored in the dark at –80°C until use. Control liver tissues were obtained through the Liver Tissue Cell Distribution Center at the University of Minnesota. Plasma and urine samples were immediately frozen and stored in the dark at –80°C until use. These studies were made exempt by the Icahn School of Medicine at Mount Sinai Institutional Review Board.

Porphyrin Precursor and Porphyrin Isomer Quantitation

Liver tissues were homogenized in 3 v/w of chilled 50 mmol/L HEPES buffer, pH 7.5, containing 1 mmol/L EDTA and 150 mmol/L KCl and then centrifuged at 10,000*g* for 10 min at 4°C. The supernatant was placed on a VWR centrifugal filter and centrifuged at 10,000g for 10 min at 4°C. Hepatic, plasma and urinary ALA and PBG concentrations were determined by liquid chromatography–tandem mass spectrometry (LC-MS/MS), as previously described (9,10).

For porphyrin analyses, liver homogenates were deproteinized in 20% TCA/DMSO (1:1, v/v), centrifuged for 10 min at 10,000*g*, and the porphyrins in the supernatants were analyzed by ultra-performance liquid chromatography (ACQUITY UPLC®, Waters Corporation), as previously described (11).

ALAS1 and HMB Synthase Enzyme Activity Assays

ALAS1 and HMB synthase activities were determined in homogenized livers as previously described (9,11). Uroporphyrin fluorescence was measured in a Foci Farrand Spectrofluorometer System 3 (Farrand Optical Components and Instruments).

Microsomal Heme Content and Cytochrome P450 (CYP) Activity Assays

Liver microsomes were isolated as previously described (12), and total protein content of the purified microsomes was determined by using the Bio-Rad DC Protein Assay Kit. Heme content was determined by using the pyridine hemochrome method of Berry and Trumpower (13). CYP2E1 activity was determined as described (12), whereas CYP1A2 activity was measured by using the P450-Glo CYP1A2 Assay kit (Promega) according to the manufacturer's instructions. Combined activity of CYP1A1, CYP1B1 and CYP3A7 was determined using the Promega P450-Glo CYP1A1/CYP1B1 Assay kit, which uses luciferin-6′ chloroethyl ether as a substrate.

Hepatic Iron Quantitation

Liver samples were dried in an 80°C oven until a constant weight was attained on two consecutive readings and then digested by using 30% high-purity hydrogen peroxide (GFS Chemicals), as previously described (14). The digested tissues were dissolved in 1% ultra-pure

nitric acid (Sigma-Aldrich), and iron concentrations were determined by graphite furnace–atomic absorption spectrophotometry (GF-AAS) by using a Varian Instruments Model-240Z Zeeman atomic absorption spectrophotometer (Varian, Inc.) equipped with a Varian GTA-120 graphite tube analyzer, a PSD-120 programmable sample dispenser and a Varian UltrAA high-intensity boosted hollow cathode lamp. The instrument and furnace settings used are provided in Supplementary Table S1. Data acquisition was carried out with the Varian SpectrAA software, and hepatic iron content was expressed as μg/mg dry tissue weight. To minimize external metal contaminations, all procedures were performed in a clean environment and autosampler cups were treated with 1% ultra-pure nitric acid and washed with ddH_2O before use.

RNA Extraction and Real-Time PCR Quantification

RNA isolation, reverse transcription and real-time polymerase chain reaction (PCR) were performed as previously described (9), by using predesigned Taqman® assays (Life Technologies) for *ALAS1* (assay ID: Hs00963534_m1), *HO-1* (Hs01110251_m1), interleukin (IL)-1β (*IL-1β*; Hs01555410_m1), IL-6 (*IL-6*; Hs00985639_m1), tumor necrosis factor α (*TNFα*; Hs01113624_g1) and glyceraldehyde 3-phosphate dehydrogenase (*GAPDH*; Hs02758991_g1). Relative *ALAS1*, *HO-1*, *IL-1β*, *IL-6* and *TNFα* transcript levels were determined by the comparative C_t method using *GAPDH* as an internal control. To validate the Taqman assay for *HO-1*, Huh-7 cells were cultured in Dulbecco modified Eagle medium supplemented with 10% fetal bovine serum and 1% penicillin-streptomycin, plated into six-well plates, and incubated for 24 h with or without 10 μmol/L hemin (Sigma-Aldrich), a potent inducer of *HO-1* expression. Relative *HO-1* mRNA levels were determined, and increased *HO-1* expression was confirmed in the hemin-treated cells.

Western Blot Analyses

ALAS1 Western blot analysis was performed as previously described (9), with the following modifications. Liver samples were homogenized in chilled lysis buffer (20 mmol/L HEPES, 150 mmol/L sodium chloride, pH 7.4, 0.2% IGEPAL, 0.5% Triton X-100 and protease inhibitor cocktail [Sigma-Aldrich]), and protein concentrations were determined using the Bio-Rad Protein Assay Dye Reagent Concentrate kit. After separation and transfer of the proteins, the polyvinylidene difluoride membranes were blocked with 5% nonfat dry milk in phosphate-buffered saline with 0.1% Tween-20 for 1 h at room temperature, incubated with anti-ALAS1 antibody (1:2,000 dilution; Fitzgerald Industries International) for 1 h at room temperature and were then incubated with horseradish peroxidase (HRP)-conjugated anti-rabbit IgG antibody (1:20,000 dilution; Santa Cruz Biotechnology) for 1 h at room temperature. Signals were detected using Immobilon Western Chemiluminescent HRP Substrate (EMD Millipore, Billerica, MA, USA). The membranes were re-probed with anti–GAPDH-HRP antibody (Santa Cruz Biotechnology) to normalize loading amounts.

Pathologic Examination of Explanted Liver

Representative liver tissues were dissected and fixed in either 10% phosphate-buffered formalin for light microscopy or 3% glutaraldehyde in 0.2 mol/L sodium cacodylate buffer for electron microscopy. Formalin-fixed livers were embedded in paraffin, cut into 4–6-μm sections and stained with hematoxylin and eosin, Masson trichrome or Perls stain. Images were captured by a Nikon DS-L1 Camera Control Unit (Nikon Corporation) attached to a Nikon Eclipse Ci light microscope (Nikon Corporation). Liver tissues fixed in glutaraldehyde were embedded in Embed 812 and cut into ultrathin sections, stained with uranyl acetate and lead citrate and then observed on a Hitachi H-7650 transmission electron microscope.

All supplementary materials are available online at www.molmed.org.

RESULTS

Case Summary

A 36-year-old Caucasian woman diagnosed with AIP at age 27 years (*HMBS* gene mutation, c.517C>T [p.Arg173Trp]) had onset of recurrent and debilitating acute attacks at age 25 years. She developed complications, including chronic axonal polyneuropathy and motor paresis. During the 5-year period before transplantation, she received a total of 267 hemin (Panhematin®) infusions (73,743 mg hemin, corresponding to 6,320 mg iron), of which 116 infusions (35,993 mg hemin, corresponding to 3,232 mg iron) were administered during the 18 months before OLT. Her course was complicated by multiple infusion port infections. She became increasingly disabled and depressed and developed chronic abdominal, back and lower-extremity pain that required continued high doses of opioid analgesics, including hydromorphone and fentanyl. Because the patient's symptoms became completely refractory to hemin, the infusions were discontinued 12 wks before transplantation. She was unable to work or to complete her college education because of continuous symptoms. After 13 months of nearly continuous hospitalization, OLT was considered.

Because AIP does not involve impairment of vital liver functions, conventional scoring systems for organ allocation were not applicable. Her case was reviewed by the regional review board for allocation of priority point exceptions. An initial model for end-stage liver disease (MELD) score of 25 was requested, with the plan to apply for higher priority points every 90 d if the patient's clinical condition did not improve. Over the following 3 months, the patient's condition worsened, requiring her to remain hospitalized for symptom management, including intravenous analgesia and antiemetics. After serial appeals to the regional review board, a final priority MELD score of 35 was obtained and transplantation was

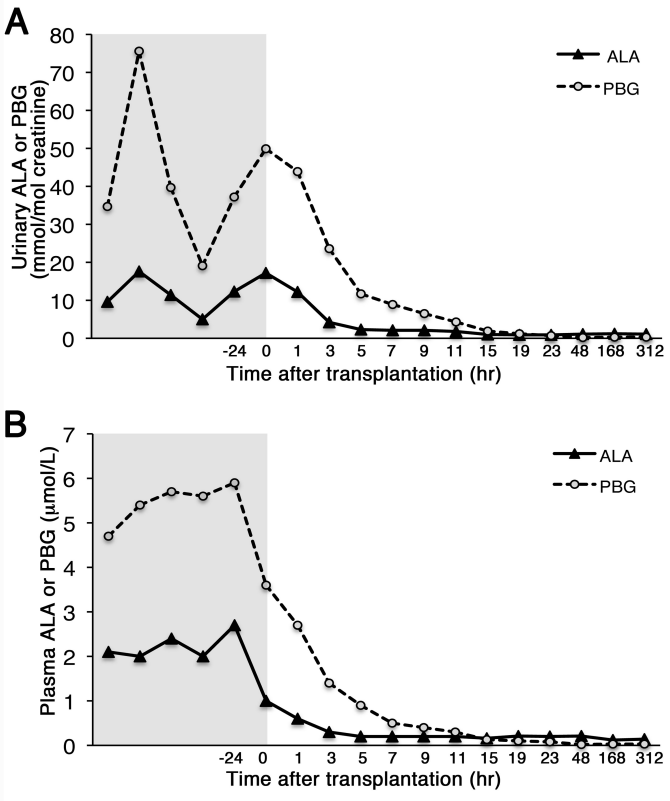

Figure 1. Liver transplantation rapidly normalized the plasma and urinary porphyrin precursor concentrations. ALA and PBG concentrations in the urine (A) and plasma (B) are shown. Pretransplantation data, shown in the shaded area, were collected 24 h before the procedure (–24) and at other time points within 4 wks of pretransplantation.

performed. The patient received a cadaveric liver from a 49-year-old male donor who died from a stroke. The cold ischemia time was 4.5 h.

On the basis of previous reports of a high incidence of hepatic arterial thrombosis after OLT in AIP patients (3), anticoagulation therapy was initiated immediately after transplantation. No complications occurred during or after the surgical procedure, and transfusions from the blood bank were unnecessary. The debilitating abdominal pain resolved immediately after transplantation, and her quality of life improved significantly. She was treated with immunosuppressive therapy including tacrolimus, prednisone and mycophenolate and was maintained on tacrolimus after mycophenolate and prednisone were tapered and discontinued at 9 and 14 months posttransplantation, respectively. She resumed full daily activities and returned to college 4 months posttransplantation. At 24 months posttransplantation, the patient continued to do well and had no acute attacks. Her neuropathic bilateral leg pain markedly improved, and although her mid-back pain attributed to porphyric nerve damage persisted, she continued to function well with multimodal pain treatment, including low-dose chronic opioid therapy. Her weight before OLT had increased to 92.9 kg (BMI 38.9 kg/m^2) because of prolonged hospitalizations and dextrose infusions. One year after transplantation, she reduced her weight to 55.2 kg (BMI 22.9 kg/m^2).

Pre- and Posttransplantation Porphyrin Precursor Studies

The patient's pretransplantation urinary ALA and PBG concentrations were markedly elevated: ALA ranging from 4.0 to 17.6 mmol/mol creatinine (norm <3.0) and PBG from 14.2 to 75.6 mmol/mol creatinine (norm <1.1). Urinary ALA and PBG normalized by 5 and 23 h posttransplantation, respectively (Figure 1A). Similarly, plasma ALA and PBG levels that were elevated before transplant, 2.0–2.7 μmol/L (norm <0.2) and 4.7–5.9 μmol/L (norm <0.05), normalized by 5 and 31 h posttransplantation, respectively (Figure 1B).

Biochemical Studies of the AIP Liver

***ALAS1* and *HO-1* expression levels.** *ALAS1* mRNA quantified by real-time PCR was approximately three-fold increased in the explanted AIP liver compared with mean levels from five "normal" control specimens (Figure 2A). Western blot analyses revealed markedly increased ALAS1 protein levels in the AIP liver relative to controls (Figure 2B), and ALAS1 enzymatic activity was 144 ± 2.5 pmol/h/mg protein, approximately five-fold greater than the mean control level of 26 ± 9.6 pmol/h/mg protein (Figure 2C). Notably, mRNA expression of heme oxygenase 1 (*HO-1*) was increased in the AIP liver by approximately three-fold relative to the control specimens (Figure 2D).

HMB synthase activity. Mean HMB synthase activity in the AIP liver was 2.5 ± 0.6 nmol/h/mg protein, whereas that in the control livers was 5.9 ± 2.4 nmol/h/mg protein. Thus, the explanted AIP liver had ~42% HMB synthase activity compared with the mean control activity (Table 1).

Porphyrin precursor and porphyrin levels. The ALA and PBG concentrations in the AIP liver were markedly increased to 58 and 4,442 pmol/mg protein, which was about 3- and 1,780-fold higher than those of the respective mean control levels of 20 and 2.5 pmol/mg protein (Table 2). Uroporphyrin I and coproporphyrin I isomers were both elevated approximately three-fold compared with the mean control values 38 versus 12 and 24 versus 8.1 pmol/g tissue, respectively (Table 2). Uroporphyrin III concentrations, which were undetectable in control

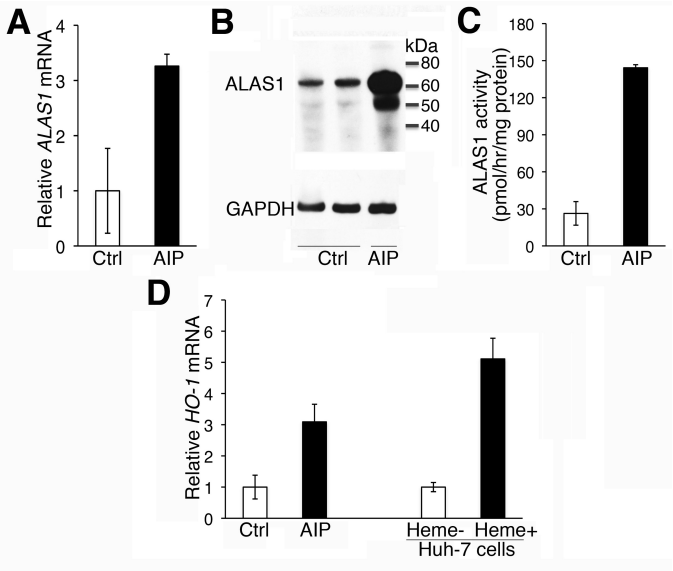

Figure 2. Hepatic *ALAS1* and *HO-1* were induced in the AIP liver. Hepatic *ALAS1* mRNA (A), protein expression levels (B) and enzymatic activities (C), as well as *HO-1* mRNA levels (D), were determined in the AIP (n = 1) and control livers (ctrl) (n = 5). In (D), the relative HO-1 mRNA level in Huh-7 cells that were incubated for 24 h with 10 μmol/L hemin, an inducer of *HO-1* expression, served as a positive control. In (A), (C) and (D), data are presented as means ± standard deviations (SDs) of three technical replicates. (B) shows a representative Western blot with two different control livers.

livers, were elevated to 20 pmol/g tissue in the AIP liver, whereas protoporphyrin IX concentrations were similar in the AIP and control livers (Table 2).

Microsomal heme content and CYP activities. To evaluate hepatic heme status, microsomal heme content and the catalytic activities of selected CYP hemoproteins were determined. Microsomes isolated from the AIP liver contained 1.5 ± 0.3 nmol/mg protein of heme, ~1.8-fold over the mean level in the controls, which was 0.8 ± 0.3 nmol/mg protein (Table 3). In the AIP liver, the CYP1A2 and CYP2E1 activities were 116 ± 2.8 relative luciferase units (RLUs)/μg protein and 1.1 ± 0.09 nmol/min/mg protein, which were comparable to the mean levels from control livers of 105 ± 20 RLU/μg protein and 1.26 ± 0.3 nmol/min/mg protein, respectively (Table 3). The combined activity of CYP1A1, CYP1B1 and CYP3A7 in the AIP liver was 4,580 ± 15 RLU/μg protein, lower than the mean level in the controls, which was 6,050 ± 310 RLU/μg protein (Table 3). However, this result was due to one of the control samples having markedly elevated activity; the activity in the AIP liver was comparable to that in the remaining four controls (Supplementary Figure S1).

Iron content. Hepatic iron concentration in the AIP liver was 2.87 μg iron/mg dry liver, which was ~5.4-fold higher than the mean control level of 0.53 μg iron/mg dry liver (Table 4), a control level comparable to literature values (15).

Table 1. HMB synthase activities in AIP and control livers.

	HMB synthase activity (nmol/h/mg protein)
Control (n = 5)	5.9 ± 2.4 (3.1–8.1)
AIP (n = 1)	2.5 ± 0.6 (1.6–3.0)

Data are means ± SD (range) derived from at least two technical replicates.

Pathological Studies of the AIP Liver

Gross pathology. The explanted liver weighed 1,550 g and measured 22 × 21 × 8 cm. The capsule had a slightly nodular appearance, although the overall texture was soft. The right lobe appeared relatively hypertrophied compared with the left. No dominant nodules were identified. Serial sectioning showed a uniformly brown cut surface with a slightly nodular appearance, but showed no apparent fibrosis, parenchymal collapse or other lesions (Figures 3A, B).

Light microscopy. Histologically, representative sections were heterogeneous. Most portal areas showed mild nonspecific lymphocytic inflammation and mild ductular reaction (Figure 3C). While bile ducts were preserved, portal vein branches were either partially or completely obliterated or dystrophic, as characterized by herniation of portal vein branches into the periportal spaces. Although the parenchyma appeared nodular, the absence of established cirrhosis was confirmed by a Masson trichrome stain. The majority of nodules

Table 2. Porphyrin precursor and porphryin levels in AIP and control livers.

Precursor/porphyrin	Controls (n = 5)	AIP (n = 1)	Fold-change over controls
ALA	20 ± 4.6	58 ± 5.1	2.9
PBG	2.5 ± 1.7	4,442 ± 162	1,777
URO I	12 ± 6.6	38	3.2
URO III	ND	20	—
COPRO I	8.1 ± 13	24	3.0
COPRO III	0.7 ± 1.1	ND	—
PROTO IX	13 ± 12	11	0.8

Data are means ± SDs. Only means are provided for porphyrin levels in AIP liver. ND, not detectable. Porphyrin precursor and porphyrin concentrations are expressed as pmol/mg protein and pmol/g tissue, respectively.

Table 3. Microsomal heme content and CYP activities in AIP and control livers.

	Controls (n = 5)	AIP (n = 1)
Microsomal heme content	0.80 ± 0.26	1.47 ± 0.27
CYP1A2	105 ± 20	116 ± 2.8
CYP2E1	1.26 ± 0.30	1.10 ± 0.09
CYP1A1 + CYP1B1 + CYP3A7	6,049 ± 309	4,498 ± 15

Data are means ± SDs derived from at least two technical replicates. Microsomal heme content is expressed as nmol/mg protein. CYP1A2 activity and the combined activity of CYP1A1, CYP1B1 and CYP3A7 are expressed as relative luciferase units/μg protein, while CYP2E1 activities are expressed as nmol/min/mg protein.

Table 4. Iron content in AIP and control livers.

	Hepatic iron content (μg iron/mg dry liver)
Control (n = 5)	0.53 ± 0.21 (0.25–0.77)
AIP (n = 1)	2.87

Data are means ± SD (range). For AIP liver, only the mean is provided.

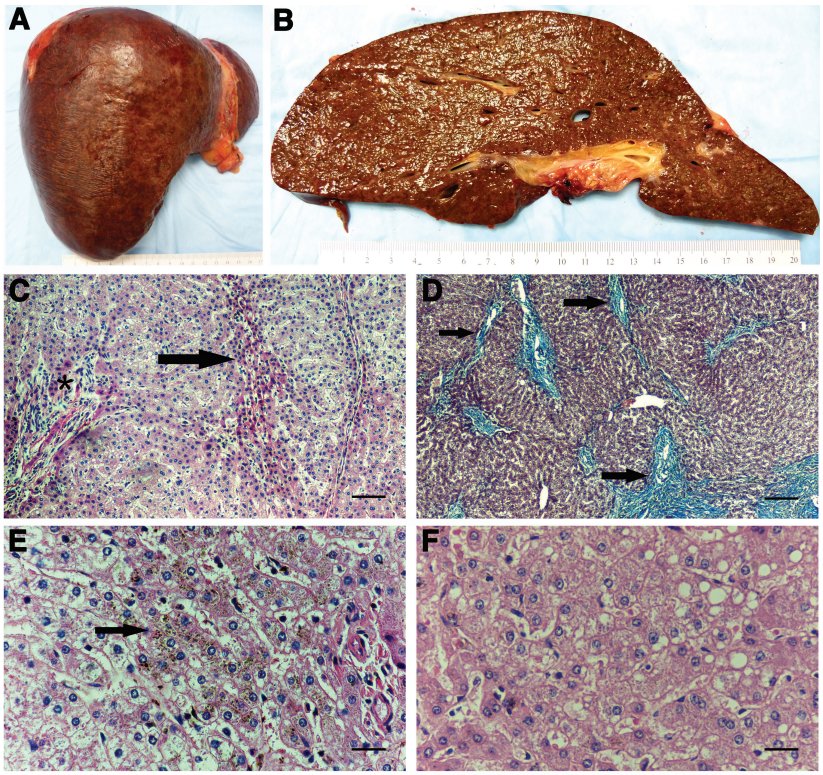

Figure 3. Pathologic findings in the AIP liver. (A) and (B) show gross liver; (C), (E) and (F) are hematoxylin and eosin stains; and (D) shows a Masson trichrome stain. (A) There is a slight nodular appearance of the capsule. No dominant lesions were identified. (B) Cut surface of the explanted liver shows a brown parenchyma with indistinct nodules and minimal fibrosis. (C) Part of a nodule wherein the portal tract is in the center (asterisk) and contains a sprinkling of mature lymphocytes with an accompanying mild ductular reaction. No interface hepatitis is seen. The arrow points to several rows of atrophic hepatocytes that act as the border of the nodule (200×). (D) An area near the hilum showing atrophy of the parenchyma, as evidenced by the approximation of portal tracts. These portal areas, indicated by arrows, are fibrotic with fibrous septa that occasionally bridge and form incomplete nodules. Portal vein branches are obliterated in this photomicrograph (200×). (E) A centrilobular zone showing dark brown pigment granules (lipofuscin) deposited within the cytoplasm of the hepatocytes. Deposition is most prominent in the area indicated by the arrow (400×). (F) Mild steatosis in the form of small and medium droplets is patchy (400×). Scale bars for (C) and (D) = 100 μm and for (E) and (F) = 50 μm.

were composed of hyperplastic hepatocytes, and the periphery of these nodules consisted of atrophic plates (Figure 3C). However, some sections taken from close to the hilum showed incomplete nodules consisting of atrophic parenchyma that were partially or completely surrounded by delicate bridging fibrous septa (Figure 3D). Most of the fibrosis occurred in the portal areas. The hepatic parenchyma had a brownish appearance at low power, due to coarse brown intracytoplasmic granules that were most prominent in centrilobular hepatocytes (Figure 3E). This pigment resembled lipofuscin, although slightly coarser in texture. Also seen was patchy steatosis ranging from focal to moderate in degree (Figure 3F). The steatotic vacuoles were mainly small droplets admixed with a few medium-sized droplets. Features of steatohepatitis were absent. Minimal iron deposition was detected by Perls stain. The main findings were nodular regenerative hyperplasia (NRH) with features of focal incomplete septal cirrhosis, mild steatosis and lipofuscin pigment deposition.

Electron microscopy. Ultrastructurally, the liver had a relatively normal histoarchitecture with generally normal peroxisomes, endoplasmic reticulum and mitochondria, although some focal hepatocytes had enlarged mitochondria. There was some cytoplasmic neutral lipid in hepatocytes and an occasional crystalline structure resembling cholesterol crystals. Kupffer cells, and possibly endothelial cells, had many electron-dense lysosomal granules. The majority of these granules were lamellar, corresponding to lipofuscin, whereas a much

smaller number were densely granular, consistent with iron deposition.

DISCUSSION

It is estimated that approximately 10% of AIP heterozygotes develop acute porphyric attacks (1). Of these individuals, ~90% are women who have cyclic attacks during the luteal phase of their menstrual cycles or even more frequent attacks (1,7,16). Certain *HMBS* genotypes were found to be more frequent among AIP heterozygotes who have recurrent attacks, including c.517C>T (p.Arg173Trp), c.518G>A (p.Arg173Gln) and c.673C>T (p.Arg225Ter) (17). Here, we report a woman with the *HMBS* p.Arg173Trp mutation whose recurrent and debilitating attacks became refractory to hemin infusions, leading to OLT. After OLT, the recurrent acute attacks stopped immediately and have not recurred for over 24 months. Moreover, her abdominal pain resolved rapidly and her peripheral neuropathy significantly improved. Her plasma and urinary ALA and PBG concentrations normalized by 5 and 31 h posttransplantation (Figures 1A, B), respectively, more rapidly than previously reported. The slower clearance of the elevated PBG relative to ALA presumably reflected the fact that pretransplantation plasma and urinary PBG levels were markedly more elevated (940- to 1,180-fold and 13- to 69-fold over normal values, respectively) than the ALA levels (10- to 14-fold and 1.5- to 6-fold over normal, respectively).

Of particular note were the biochemical and pathologic studies of the explanted porphyric liver. Hepatic *ALAS1* expression was increased (Figures 2A–C), consistent with the increased levels of ALA and PBG. Notably, hepatic ALA was only moderately elevated (~3-fold) compared with the dramatically elevated hepatic PBG levels (~1,780-fold; Table 2), indicating that ALA overproduced in the liver was either rapidly released into the circulation for excretion or metabolized to PBG by the abundant hepatic ALA-dehydratase activity. HMB synthase activity was ~42% compared with the mean activity in control livers (Table 1), consistent with the previous finding that prokaryotic expression of the p.Arg173Trp *HMBS* allele resulted in <1% residual HMB synthase activity (18). That the HMB synthase activity was approximately half-normal argued against the previously proposed hypothesis that the elevated PBG may significantly decrease the half-normal HMB synthase activity during an acute attack via substrate inhibition (7). The hepatic uroporphyrin III concentration was elevated approximately three-fold over the mean value in control livers, indicating that sufficient PBG was converted to hydroxymethylbilane despite the half-normal HMB synthase activity (Table 2). Moreover, microsomal heme content was increased compared with the mean level in the control livers, and the catalytic activities of several CYP450 enzymes (CYP1A2, CYP2E1, and CYP1A1 + CYP1B1 + CYP3A7) were within the normal range in the AIP liver (Table 3 and Supplementary Figure S1). Thus, abdominal pain (the most common acute attack symptom) occurred in the presence of increased hepatic *ALAS1* expression and markedly elevated hepatic and circulating ALA and PBG levels, but in the absence of generalized hepatic heme deficiency. These findings suggest that the hepatic heme deficiency in AIP is confined to depletion of the "free" heme pool, leading to greater induction of *ALAS1* and accumulation of the putatively neurotoxic ALA and/or PBG. Importantly, these findings validate the use of a liver-directed RNA interference (RNAi) therapeutic targeting hepatic *ALAS1* mRNA for the prevention and treatment of acute attacks, as shown in recent preclinical studies (9).

The expression of *HO-1*, the first and rate-limiting enzyme in heme catabolism, also was induced in the AIP liver (Figure 2D). *HO-1* can be induced at the transcriptional level by heme accumulation, as well as by various cellular stresses, including inflammatory cytokines, hypoxia and oxidative stress (19). Increased HO-1 activity has antioxidant and antiinflammatory effects and plays a cytoprotective role under stress conditions (19). Our transplant recipient did not receive therapeutic hemin for 3 months before OLT, thereby excluding exogenous heme as a mechanism of *HO-1* induction. As microsomal heme content was elevated in the AIP liver relative to mean control levels (Table 3), it is possible that hepatic *HO-1* expression was induced as a result of increased endogenous heme production. Alternatively, *HO-1* expression may have been elevated as a result of the chronic nonspecific portal inflammation and/or incomplete septal cirrhosis, as evidenced by the explant's pathological examination (Figures 3C, D). Indeed, the mRNA expression of proinflammatory cytokines *IL-1β*, *IL-6* and *TNFα* were elevated in the AIP liver compared with mean control levels (Supplementary Table S2). The upregulated HO-1 activity may have exacerbated porphyric symptoms, as the increased heme degradation may contribute to elevated levels of the putatively neurotoxic ALA and PBG by increasing the transcriptional activity of *ALAS1* (20,21) and the import of precursor ALAS1 into the mitochondria, where the protein is converted to its mature form (22).

To date, the few studies of AIP liver pathology describe nonspecific findings, including minimal to moderate steatosis, hemosiderosis and lipofuscinosis (3,23–28). None of the previously reported cases described the NRH or incomplete septal cirrhosis seen in our patient (Figures 3C, D). NRH and incomplete septal cirrhosis both involve vascular obstruction of small hepatic arteries or portal branches and may progress to noncirrhotic portal hypertension. NRH is typically associated with systemic autoimmune diseases, hematological disorders and various drugs, particularly immunosuppressant and chemotherapeutic agents (29,30), whereas incomplete septal cirrhosis has been described in patients with viral hepatitis, alcoholism and exposure to vasculotoxic chemicals such as arsenic (31). Our patient did not have any of

these conditions, nor was she on medication known to induce NRH or incomplete septal cirrhosis. It is possible that AIP itself may have led to these pathologic changes, although there is no known association between AIP and hepatic vascular injury or an intrahepatic hypercoaguable state. While it is uncommon for NRH, characterized by a lack of fibrosis, and incomplete septal cirrhosis to coexist within the same liver, such cases have been reported (32).

Also notable was the observation that hepatic iron deposition was minimal in the AIP liver, despite the remarkable number of hemin infusions during the 5 years pretransplantation. In line with this finding, the patient's hepatic iron content was only mildly elevated (~5-fold) compared with the control livers (Table 4), and the patient's ferritin did not exceed 760 ng/mL, even during the time she was receiving frequent hemin infusions. These findings suggest that hemin-induced iron overload most likely was not a contributing mechanism to the hepatic architectural changes, including NRH and fibrosis.

CONCLUSION

These studies document the first OLT in the Americas in a severely affected AIP patient that resulted in the rapid clearance of the accumulated ALA and PBG, prevented further acute attacks and ameliorated chronic neuropathic pain. Biochemical studies of the explanted AIP liver provided important insights into the disease pathogenesis, indicating that (a) the acute and persistent neurovisceral pain in AIP is most likely associated with depletion of the hepatic "free" heme pool, but not with generalized hepatic heme deficiency, and (b) substrate inhibition of hepatic HMB synthase activity by PBG is not a likely pathogenic mechanism in the acute attacks. Although OLT is potentially curative, it is associated with high morbidity and limited organ availability and should be reserved as a last resort therapy for AIP patients with intractable, severe and frequent neurovisceral manifestations. Future novel therapeutic approaches that are safe and effective are desirable for the prevention and treatment of the acute porphyric attacks.

ACKNOWLEDGMENTS

We thank Ethellyn Panta (Icahn School of Medicine at Mount Sinai) and Hector Bergonia (University of Utah School of Medicine) for their excellent technical assistance. This work was supported in part by Career Development Awards K01 DK087971 (to M Yasuda) and K23 DK095946 (to M Balwani) from the National Institutes of Health (NIH) and a cooperative grant (U54 DK083909) for the Porphyrias Consortium, which is a part of the NIH Rare Diseases Research Network (RDCRN) and supported through collaboration between the NIH Office of Rare Diseases Research (ORDR) at the National Center for Advancing Translational Science (NCATS) and National Institute of Diabetes and Digestive and Kidney Diseases (NIDDK). The content is solely the responsibility of the authors and does not necessarily represent the official views of the NIH. The Liver Tissue Cell Distribution System at the University of Minnesota provided the control human liver tissues and is funded by NIH contract HHSN276201200017C.

DISCLOSURE

M Yasuda and RJ Desnick received research support from Alnylam Pharmaceuticals and are inventors on intellectual property licensed through the Icahn School of Medicine at Mount Sinai to Alnylam Pharmaceuticals. RJ Desnick is a consultant for Recordati Rare Diseases and Alnylam Pharmaceuticals. KE Anderson is a consultant for Mitsubishi Tanabe Pharma America.

REFERENCES

1. Anderson KE, Sassa S, Bishop DF, Desnick RJ. (2001) Disorders of heme biosynthesis: X-linked sideroblastic anemia and the porphyrias. 8th edition. 8th edition. In: *The Metabolic and Molecular Bases of Inherited Disease*. Scriver CR, Beaudet AL, Sly WS, Valle D, Childs B, Kinzler KW, Vogelstein B (eds.) McGraw-Hill, New York, pp. 2961–3062.
2. Dar FS, *et al.* (2010) Liver transplantation for acute intermittent porphyria: a viable treatment? *Hepatobiliary Pancreat. Dis. Int*. 9:93–6.
3. Dowman JK, *et al.* (2012) Liver transplantation for acute intermittent porphyria is complicated by a high rate of hepatic artery thrombosis. *Liver Transpl*. 18:195–200.
4. Seth AK, Badminton MN, Mirza D, Russell S, Elias E. (2007) Liver transplantation for porphyria: who, when, and how? *Liver Transpl*. 13:1219–27.
5. Soonawalla ZF, *et al.* (2004) Liver transplantation as a cure for acute intermittent porphyria. *Lancet*. 363:705–6.
6. Wahlin S, *et al.* (2010) Combined liver and kidney transplantation in acute intermittent porphyria. *Transpl. Int*. 23:e18–21.
7. Harper P, Sardh E. (2014) Management of acute intermittent porphyria. *Expert Opin. Orphan Drugs*. 2:349–68.
8. Dowman JK, Gunson BK, Bramhall S, Badminton MN, Newsome PN. (2011) Liver transplantation from donors with acute intermittent porphyria. *Ann. Intern. Med*. 154:571–2.
9. Yasuda M, *et al.* (2014) RNAi-mediated silencing of hepatic Alas1 effectively prevents and treats the induced acute attacks in acute intermittent porphyria mice. *Proc. Natl. Acad. Sci. U. S. A.* 111:7777–82.
10. Zhang J, *et al.* (2011) A LC-MS/MS method for the specific, sensitive, and simultaneous quantification of 5-aminolevulinic acid and porphobilinogen. *J. Chromatogr. B Analyt. Technol. Biomed. Life Sci*. 879:2389–96.
11. Clavero S, *et al.* (2010) Feline acute intermittent porphyria: a phenocopy masquerading as an erythropoietic porphyria due to dominant and recessive hydroxymethylbilane synthase mutations. *Hum. Mol. Genet*. 19:584–96.
12. Wu D, Cederbaum AI. (2008) Development and properties of HepG2 cells that constitutively express CYP2E1. *Methods Mol. Biol*. 447:137–50.
13. Berry EA, Trumpower BL. (1987) Simultaneous determination of hemes a, b, and c from pyridine hemochrome spectra. *Anal. Biochem*. 161:1–15.
14. Alcock NW. (1987) A hydrogen-peroxide digestion system for tissue trace-metal analysis. *Biol. Trace Elem. Res*. 13:363–70.
15. Barry M. (1974) Liver iron concentration, stainable iron, and total body storage iron. *Gut*. 15:411–5.
16. Bonkovsky HL, *et al.* (2014) Acute porphyrias in the USA: features of 108 subjects from porphyrias consortium. *Am. J. Med*. 127:1233–41.
17. von und zu Fraunberg M, Pischik E, Udd L, Kauppinen R. (2005) Clinical and biochemical characteristics and genotype-phenotype correlation in 143 Finnish and Russian patients with acute intermittent porphyria. *Medicine (Baltimore)*. 84:35–47.
18. Solis C, *et al.* (2004) Acute intermittent porphyria: studies of the severe homozygous dominant disease provides insights into the neurologic attacks in acute porphyrias. *Arch. Neurol*. 61:1764–70.
19. Srisook K, Kim C, Cha YN. (2005) Molecular

mechanisms involved in enhancing HO-1 expression: de-repression by heme and activation by Nrf2, the "one-two" punch. *Antioxid. Redox Signal*. 7:1674–87.
20. Gotoh S, Nakamura T, Kataoka T, Taketani S. (2011) Egr-1 regulates the transcriptional repression of mouse delta-aminolevulinic acid synthase 1 by heme. *Gene*. 472:28–36.
21. Yamamoto M, Kure S, Engel JD, Hiraga K. (1988) Structure, turnover, and heme-mediated suppression of the level of mRNA encoding rat liver delta-aminolevulinate synthase. *J. Biol. Chem.* 263:15973–9.
22. Lathrop JT, Timko MP. (1993) Regulation by heme of mitochondrial protein transport through a conserved amino acid motif. *Science*. 259:522–5.
23. Biempica L, Kosower N, Ma MH, Goldfischer S. (1974) Hepatic porphyrias: cytochemical and ultrastructural studies of liver in acute intermittent porphyria and porphyria cutanea tarda. *Arch. Pathol*. 98:336–43.
24. Heilmann E, Muller KM, Niedorf H, Bassewitz DB. (1976) Special clinical, light and electron microscopic aspects of acute intermittent porphyria. *Ann. Clin. Res*. 8 Suppl 17:213–6.
25. Jean G, Levi L, Ranzi T. (1967) Hepatic siderosis in porphyria cutanea tarda [Clinical and pathogenetic considerations]. *G. Ital. Dermatol. Minerva Dermatol*. 108:507–24.
26. Ostrowski J, *et al.* (1983) Abnormalities in liver function and morphology and impaired aminopyrine metabolism in hereditary hepatic porphyrias. *Gastroenterology*. 85:1131–7.
27. Perlroth MG, *et al.* (1966) Acute intermittent porphyria: new morphologic and biochemical findings. *Am. J. Med*. 41:149–62.
28. Suarez JI, *et al.* (1997) Acute intermittent porphyria: clinicopathologic correlation: report of a case and review of the literature. *Neurology*. 48:1678–83.
29. Al-Mukhaizeem KA, Rosenberg A, Sherker AH. (2004) Nodular regenerative hyperplasia of the liver: an under-recognized cause of portal hypertension in hematological disorders. *Am. J. Hematol*. 75:225–30.
30. Hartleb M, Gutkowski K, Milkiewicz P. (2011) Nodular regenerative hyperplasia: evolving concepts on underdiagnosed cause of portal hypertension. *World J. Gastroenterol*. 17:1400–9.
31. Schinoni MI, Andrade Z, de Freitas LA, Oliveira R, Parana R. (2004) Incomplete septal cirrhosis: an enigmatic disease. *Liver Int*. 24:452–6.
32. Le Bail B, *et al.* (1997) Case report: incomplete septal cirrhosis with liver cell dysplasia. *J. Gastroenterol. Hepatol*. 12:267–71.

Cite this article as: Yasuda M, *et al*. (2015) Liver transplantation for acute intermittent porphyria: biochemical and pathologic studies of the explanted liver. *Mol. Med*. 21:487–95.